Kinetic roughening of the interfaces of Langmuir-Blodgett films

Xiu-Hong Li, Ming Li,* and Zhen-Hong Mai
Institute of Physics, Chinese Academy of Sciences, Beijing 100080, People's Republic of China
(Received 24 December 2003; revised manuscript received 2 March 2004; published 18 June 2004)

We report x-ray scattering and atomic force microscopy measurements on the interfacial roughening of cadmium stearate Langmuir-Blodgett (LB) films of different total thickness. It is shown that the growth front becomes rougher as the film grows thicker. The initial sublayers in the films follow the fluctuations of the substrate. However, intrinsic roughening induced by pinholes shows up very soon so that the interfaces eventually exhibit logarithmic correlation. All experiments are explained quantitatively using the correlation function derived from a recently proposed growth equation for imperfect LB films. This supports the idea that the interfacial morphology in LB films is determined by the competition between the roughening arising from pinholes and the smoothening due to the surface tension of the membranes.

DOI: 10.1103/PhysRevB.69.235407 PACS number(s): 68.47.Pe, 81.15.Aa, 61.10.Kw, 68.55.−a

I. INTRODUCTION

Langmuir-Blodgett (LB) films have been studied extensively for decades due to their potential applications in molecular electronics, nonlinear optics, biosensors, and so on.[1] They are prepared layer by layer by transferring Langmuir layers already formed on a liquid subphase onto a solid surface.[2] The transfer is usually quantified by a parameter called transfer ratio, which is defined as the ratio of the area swept by a moving barrier during the transfer of a single monolayer to the area of film deposition on the substrate.[3] In a nonideal transfer process desorption may occur, leaving the surface with many holes, and the transfer ratio is thus less than unity. A subsequently deposited monolayer is forced to follow the fluctuations created by the holes, resulting in rough interfaces. One expects that the imperfections will be transferred from one layer to the next. However, questions concerning the degree of conformality, the detailed morphology of the interfaces, and the possible evolution of the roughness from the substrate to the top layers are still to be addressed.[4] In this paper, we focus on these questions by studying the interfaces of a series of LB films with increasing the total number of layers.

The techniques we used in this study include atomic force microscopy (AFM) and x-ray scattering. AFM emerged recently as a very powerful structural probe, giving information in real space for practically all types of surfaces.[5] In addition to atomic resolution images of surfaces, one can obtain, with AFM, quantitative morphological information even up to a micron length scale. For instance, it is possible to measure the local rms roughness of a surface by performing scans of different lengths. From the scaling of this measured local roughness with scan size, it is possible to get the height-difference correlation function.[6] AFM measurements are restricted to the top surface only, they provide information complementary to that obtained from the x-ray scattering. The latter has proven to be one of the most powerful and direct methods to characterize the interfacial structure of multilayered films. The specular reflectivity detects the averaged structure in the direction perpendicular to the interfaces,[7] while the transverse diffuse scattering is sensitive to the lateral structure of the interfaces.[8] The diffuse scattering of a multilayered system is a unique transformation of the statistical height-difference correlation function defined as $g_{ij}(r)=\langle[h_i(0)-h_j(r)]^2\rangle$, where h denotes the deviation from the mean position of the interfaces labeled by i or j.[8]

Many efforts have contributed to determine the correlation function of multilayered systems.[9–11] The correlation function contains information about the degree of conformality of the interfaces. For example, the correlation function $g_{ij}(r)$ for a film whose interfaces are totally conformal is independent of the subscripts i or j. More importantly, success in obtaining the correlation function would help to have access not only to the spatial, but also to the temporal aspects of the growth process, as different interfaces can be attributed to different times during growth.

Although the application of x-ray diffraction to the LB films can be dated back to as early as 1930s, when Holly and Bernstein performed the first x-ray analysis of an LB film prepared by Blodgett,[12] only very recently has the diffuse scattering technique begun to attract attention of the researchers working in this field.[2,4,13,14] A remarkable progress was recently made by Gibaud *et al.*, who found evidence of self-affine rough interfaces in LB films.[15] This result encourages one to suspect that statistical models are applicable for the interfaces even in systems consisting of rod-like molecules.[4] Recently, evidence of another kind of scaling, namely, the logarithmic scaling of the LB interface, was given by Basu *et al.*[2] In many of the studies on LB films so far, it was assumed that the interfaces are completely conformal so that a single correlation function is enough to explain the diffuse scattering curves.[2,15] However, this is unsuitable for most cases.[16,17] Nitz *et al.* therefore proposed a correlation function in which a vertical correlation length was introduced to characterize the partial conformality of the interfaces.[4] Although it worked well for their data and has become popular in the x-ray community, it still lacks a strong physical basis in that it ignores the wavelength dependence of the conformality. Intuitively, fluctuations of one layer with very high spatial frequency will not be replicated completely by the following layers. Li *et al.* found that the aforementioned correlation functions could not explain their experimental data.[18] They derived a correlation function from an

evolution equation that describes the growth dynamics of imperfect LB films and found that only two free parameters were needed to explain their diffuse scattering data. In this work, we will show that the same correlation function can be used to explain all of our experimental data. The correlation function is in closed analytical form and is computationally efficient. A saturation phenomenon, which was taken into account by a crude introduction of correlation length in the literature, is a natural result of such a correlation function. Moreover, it contains a part that accounts for the effect of the substrate.

II. THEORETICAL BACKGROUND

Many types of differential equations have been proposed to describe the evolution of the interfacial morphology and to predict the scaling property of the interfaces.[5] A quite early effort to derive the correlation spectrum of a growing front was made by Edwards and Wilkinson,[19] who derived an equation for the deposition of *discrete* particles, given by

$$\frac{\partial h(r,t)}{\partial t} = r_D \nu_2 \nabla^2 h(r,t) + \eta(r,t), \tag{1}$$

where $h(r,t)=H(r,t)-r_D t$ with $H(r,t)$ being the film thickness at point r and at time t, r_D is the deposition rate, and ν_2 is a coefficient. The first term on the right-hand side of Eq. (1) accounts for the relaxation of the surface towards equilibrium, and the second is the noise. This equation results in logarithmic scaling of the interfacial correlation. Various growth equations have since then been proposed that have greatly deepened our understanding of the growth dynamics of thin films.[5]

By comparing the measured and the theoretically calculated scaling exponent, one can classify the growth dynamics of thin films.[20,21] X-ray scattering is one of the effective means to obtain the correlation function. In the Born approximation, the differential cross section of x-ray scattering from a multilayered system on a solid surface is written as[9,22]

$$\frac{d\sigma}{d\Omega} \propto \sum_{i,j=0}^{N} f_i f_j^* e^{iq_z(z_i - z_j)} \int e^{-q_z^2 g_{ij}(r)/2} e^{iq_r r} d^2 r, \tag{2}$$

where z_i denotes the position of interface i, and f_i is the reflection of layer i. The scattering of the whole substrate has been absorbed into f_0. Equation (2) applies to the LB films as well. For example, Gibaud *et al.* found that a self-affine correlation can interpret the diffuse scattering data of their LB films.[15] A recent breakthrough was made by Basu *et al.*, who found via x-ray scattering that the interfaces of their LB films scale in either a logarithmic or a self-affine manner, depending on the substrate on which the LB films are deposited.[2] They proposed that the growth of the LB films can be described by

$$\frac{\partial h}{\partial t} = \nu \nabla^2 h - \Lambda \nabla^4 h + N_d + N. \tag{3}$$

The first and second terms on the right-hand side of the equation describe the adsorption/desorption process controlled by the surface tension and the diffusion process, respectively. ν and Λ are constants related to the corresponding surface tension and the diffusion, respectively. N_d and N are, respectively, conservation and nonconservation diffusive noise. Basu *et al.* defined a length scale $\xi(\sim\sqrt{\Lambda/\nu})$ and compared it with the coherence length L_c of the x-rays in the experiments. They argued that, if $\xi \ll L_c$, the interface exhibits logarithmic correlation, while for $\xi \gg L_c$, the correlation function is found to scale in a self-affine manner. Unfortunately, they did not specify the coefficients in the equation quantitatively. In addition there was no interpretion as to why the coherence length of the x rays should be a decisive parameter. Starting from the interaction between the transferred membrane and the rough growth front, Li *et al.* derived an equation for the evolution of the interfacial morphology of LB films.[18] It reads as

$$\frac{\partial h(r)}{\partial z} = \frac{\zeta^2}{d}\nabla^2 h(r) - \frac{Y^4}{d}\nabla^4 h(r) + \frac{\eta(r,t)}{r_D}, \tag{4}$$

in which the noise $\eta(r,t)$ is explicitly included as in Eq. (1). ζ and Y are two healing lengths, characterizing the dependence of conformality on the wavelength of the fluctuations,[18] and d is the distance between two adjacent interfaces. The interfacial correlation in an LB film whose growth is described by Eq. (4) is characterized by a crossover from self-affine scaling on short length scales to logarithmic scaling on large length scales.[5] The crossover length is defined as $\delta = Y^2/\zeta$. δ is generally only a few nanometers,[18] quite smaller than the short distance cutoff in the films. The short distance self-affine scaling is thus not observable in most x-ray diffuse scattering experiments of the LB films. Y^4/d in Eq. (4) can therefore be ignored. The noise $\eta(r,t) = -\Sigma_1^N \delta(t-t_i) f_i(r-r_i)$ in Eq. (4) represents a series of random desorbing patches of shape f_i centered at position r_i and occurring at time t_i. N is the total number of events of desorption after a growth time T. The shape $f(r-r_i)$ might be some given function or it may itself be distributed with some probability functional.[19] The only important feature of $f(r-r_i)$ is that it must have a sharp cutoff at $|r-r_i|=a$, where a is the size of the patches. Equation (4) with $Y^4/d=0$ can be analytically solved if one assumes $f_i = d\exp[-(r-r_i)^2/2a^2]$. This leads to a height-difference correlation function

$$g_{ij}(r) = g_{ij}^{(0)}(r) + \pi c \frac{a^2 d}{\nu_2}\left[g_{ij}^{(\infty)}(r) - \frac{1}{2} g_{ij}^{(i)}(r) - \frac{1}{2} g_{ij}^{(j)}(r) \right], \tag{5}$$

where $c=(Na^2 d)/(r_D T A)$ is the volume concentration of the defects, which is related to the mean transfer ratio by $(1-c)$, A is the area of the surface,

$$g_{ij}^{(0)}(r) = \int \frac{d^2 q_{xy}}{2\pi^2} e^{-\nu_2 (z_i + z_j) q_{xy}^2} |u(0,q_{xy})|^2 (1 - e^{iq_{xy} r}),$$

$$g_{ij}^{(\infty)}(r) = 2\gamma_E + Ei\left(\frac{r^2}{4(a^2 + |z_j - z_i|\nu_2)} \right) + \ln\left(\frac{r^2}{4a^2} \right),$$

and

$$g_{ij}^{(j)}(r) = 2\gamma_E + Ei\left(\frac{r^2}{4[a^2 + (z_j + z_i)\nu_2]}\right) + \ln\left(\frac{r^2}{4(a^2 + 2z_j\nu_2)}\right).$$

where $\nu_2 = \zeta^2/d$, $z_i = id$ denotes the position of interface i, γ_E is the Euler Gamma constant, and $Ei(x) = \int_x^\infty t^{-1}e^{-t}dt$. The first term in Eq. (5) represents the effect of the substrate. If the surface of the substrate is self-affine, one has $|u(0,q_{xy})|^2 = \int d^2r\sigma_0^2 \exp(-(r/\xi_\parallel)^{2h})\exp(iq_{xy}r)$ where σ_0, $\xi_\parallel$, and h are the rms roughness, lateral correlation length, and the Hurst exponent, respectively.[22] The term $g^{(\infty)}(r)$ explains the asymptotic logarithmic scaling as the thickness tends to infinity. The last two terms account for the macroscopic saturation due to the finite thickness of the films.

Although the correlation function [Eq. (5)] is rather complicated, there are actually only two free fitting parameters, namely, ζ and a. The parameter c in Eq. (5) is determined by the transfer ratio, which can be measured during the film deposition, d was from the reflectivity, and σ_0, $\xi_\parallel$, and h were estimated by fitting the diffuse scattering of the substrate. It is worth noting that Eq. (4) is conceptually different from Eqs. (1) and (3), although they are very similar in mathematical formalism. Equation (1) is for deposition processes of *discrete* particles, such as in sputtering or molecular beam epitaxy growth. Equation (3) is a direct generalization of Eq. (1) and thus belongs to the same group of classical growth models for deposition of discrete particles. On the contrary, a depositing membrane is treated as a whole when deriving Eq. (4) (see Ref. 18 for more details). The two healing lengths, ζ and Y, are determined by the intrinsic elastic properties of the membranes and the strength of interaction between the transferred membranes. More importantly, it takes into account directly the growth conditions such as the transfer ratio $(1-c)$, and the effect of the substrate. In the following, we will use this correlation function to explain all of our data and will show that it is a proper correlation function for imperfect LB films.

III. EXPERIMENTS

Stearic acid, cadmium chloride, and chloroform are all analytical-reagent grade and were used as supplied. A Milli-Q water purification system (Millipore Corp.) was used to produce water with a resistivity of $1.8\times10^5\ \Omega$ m for all the experiments.

The LB films of cadmium stearate were built up in an LB trough (Nima Technology Ltd). The solution of stearic acid (in chloroform, 1 mg/ml) was spread on an aqueous solution of cadmium chloride (1 mM) at pH=6.0. The films were deposited on silicon substrate at a constant surface pressure (40 mN/m) and at a temperature of 25°C. The deposition rate was 5 mm/min. LB films of 1, 3, 5, 7, 15, and 27 monolayers (ML) were prepared.

The x-ray experiments were performed on a Bruker D8-Advance diffractometer equipped with a Goebel mirror to obtain parallel x-ray beams and to suppress the Cu K_β radiation. Cu K_α radiation was used. The incident beam was confined by a 0.1 mm slit 300 mm before the sample and the scattered beam was confined by a 0.2 mm slit. The specular reflectivity was measured by performing the $\theta/2\theta$ scan while keeping the incidence angle equal to the exiting angle. The transverse scan was performed by rocking the sample, keeping the angle between the incidence and the reflection fixed. The longitudinal diffuse scattering data were collected by performing the $\theta/2\theta$ scan while maintaining a fixed angular offset between the incidence angle and the exiting angle. The detector is wide open in the out-of-plane direction to integrate effectively the scattering perpendicular to the scattering plane (along q_y).

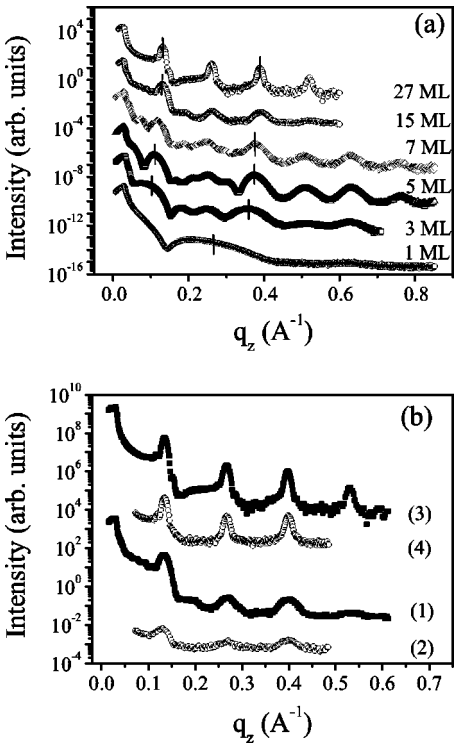

FIG. 1. (a) Reflectivity curves of the samples. (b) The specular reflectivity and the longitudinal diffuse scattering of the 15 ML film are shown as curves (1) and (2), respectively; those for the 27 ML film are shown as curves (3) and (4), respectively.

The surface topography of the samples was observed with a NanoScope IIIa (DI Co.) AFM. The images were obtained in the tapping mode in air at room temperature.

IV. RESULTS AND DISCUSSION

Shown in Fig. 1(a) are the specular reflectivity curves of the samples. Bragg peaks are observable after 5 ML deposition. The weakening of the even order Bragg peaks is due to the lower electron density between the touching hydrocarbon chains.[23] Figure 1(b) shows the longitudinal diffuse scattering data taken with a constant angular offset of 0.2° for the 15 and 27 ML films. It indicates that there exists correlated roughness fluctuation in the films. Figure 2 shows, as examples, the AFM topographic images of the 1 and 3 ML LB films. Holes formed during deposition are clearly visible. The surfaces become rougher as the films grow thicker. This supports the idea that the kinetic roughening is due to formation of holes during membrane transfer. Existence of holes in LB films has been observed for many years.[24,25] It has been

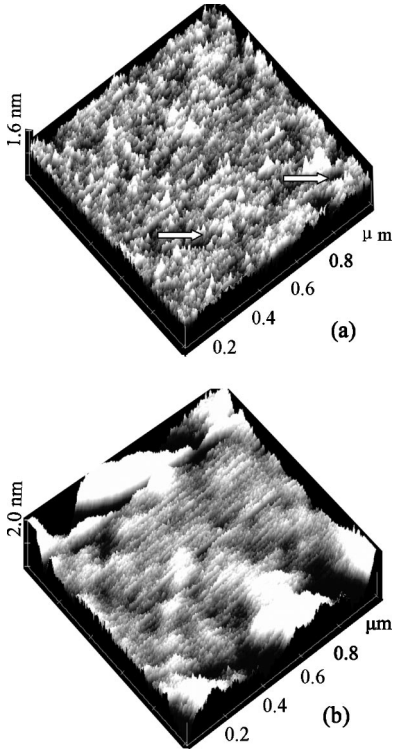

FIG. 2. AFM images of scan size 1 μm $\times$ 1 μm for the LB films of 1 ML (a) and 3 ML (b). Examples of pinholes formed during deposition are indicated by the arrowheads.

related to the balance between the adsorption energy of the molecules on the surface and their energy at the air-water interface.[3] The membranes have already formed on the surface of water before they are transferred onto a surface. Such membranes could be quite rigid so that one can even deposit a film on a wire mesh.[26] Therefore, a hole covered by membranes on top of it will soon be filled and leveled up. The layered structure is thus maintained in spite of the existence of holes. However, the sinking of the molecules right above the holes forces the membrane to fluctuate. This and the newly created holes will eventually roughen the interfaces. The scaling of the interfaces is determined by the competition between the holes that roughen the interface and the healing force due to surface tension that smoothens the interface. This idea is reflected in Eq. (4) and we believe that the correlation function [Eq. (5)] derived from it is a good candidate to be used in Eq. (2) for explaining our diffuse scattering data.

Figure 3 shows the data (circles) and fits (lines) of the transverse scans taken along q_x (in log-log plot) for the samples and the substrate. The diffuse scattering of the 1 ML LB film looks like that of the naked silicon surface. However, the diffuse scattering curves of the 27 ML film show a totally different feature. The diffuse scattering of the samples with 3–15 ML consists of two regions. The curve in the small q_x range just beyond the specular peak resembles that of the substrate. The size of this region decreases as the number of layers increases. The data in the large q_x range look like that of the 27 ML film, taking on a power-law decay in which the diffusely scattered intensity is proportional to $q_x^{-1+\eta}$. This reveals that the correlation of the interfaces eventually takes on the logarithmic character after deposition of 3 ML. The first transferred layer effectively damps the substrate roughness, and intrinsic roughening induced by pinholes shows up very soon so that the interfaces eventually exhibit logarithmic correlation. The solid lines in Fig. 3 are the theoretical fit according to Eq. (5) using the parameters listed in Table I, in which a and ζ are the only two fitting parameters. The good agreement between the measurement and the calculation is impressive. In order to show how sensitively the x-ray diffuse scattering curves are dependent on the parameters of ζ and a, we show as an example in Fig. 4 the calculated correlation function $g_{2,6}(r)$ and the corresponding diffuse scattering according to Eq. (5) for the 7 ML film with different values of ζ and a. It demonstrates that the diffuse scattering curve is sensitive to both ζ and a. We have tried to use some other correlation functions we found in the literature to fit the data. The self-affine correlation function was immediately ruled out because it predicts that the decay rate of the diffuse scattering curves is independent of the order of the Bragg peaks at which the transverse scan was made. A single correlation function used by Basu *et al.*[2] can indeed reproduce the diffuse scattering

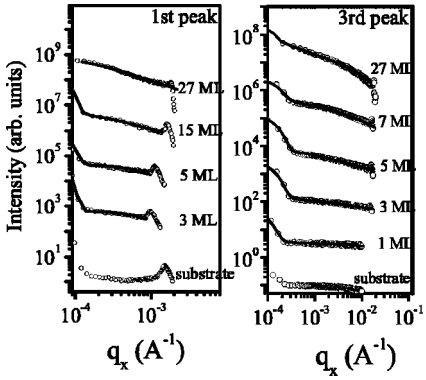

FIG. 3. Diffuse scattering at the first peak (left panel) and the third peak (right panel) for the samples are shown along with the fitted curves. The diffuse scattering curve of the substrate is also presented. The Yoneda peaks (see Ref. 8) were not included in the simulations. The exact positions at which the transverse scans were performed are indicated by small vertical bars in Fig. 1.

TABLE I. Parameters used to fit the diffuse scattering curves of the samples in which a and ζ are the only two fitting parameters. The parameter c is determined by the average transfer ratio which was measured during the film deposition.

Film thickness (ML)	ζ ($\pm$9 nm)	a ($\pm$0.5 nm)	c ($\pm$0.05)
1	111	18	0.25
3	114	16	0.29
5	112	14	0.29
7	112	15	0.30
15	112	15	0.32
27	112	15	0.32

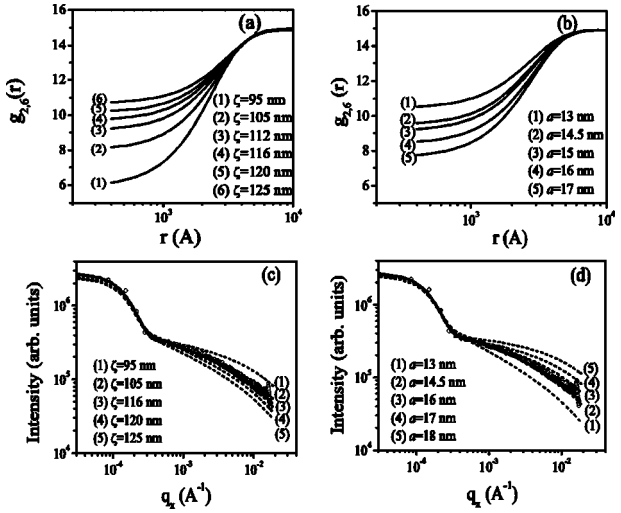

FIG. 4. Calculations according to Eq. (5) with different values of ζ and a for the film of 7 ML. (a) Calculated correlation function $g_{2,6}(r)$ with different ζ at $a=15$ nm. (b) $g_{2,6}(r)$ with different a at $\zeta=112$ nm. (c) and (d) are the corresponding diffuse scattering intensities (dashed lines). The solid lines are the best fit to the experimental data (symbols).

curve of the thickest film, but it failed to fit well the diffuse scattering data of the thinner films.

With AFM, quantitative morphological information about the statistics of surfaces can be obtained. Following Ref. 6, we calculated the height-difference correlation functions of the surface fluctuations for the 1, 3, 5, and 7 ML LB films as shown in Fig. 5. To give a convincing support to the correlation function used in this study, we compared the height-difference correlation spectra of the surfaces of the samples calculated according to Eq. (5) with the ones derived from the AFM measurements. The agreement between them is quite good. One observes that the surface of the 1 ML sample does not belong to the group of thicker films, but is similar to a featureless flat surface. This is because the silicon surface is smooth beyond its lateral correlation length $\xi_{\|}$ (here, $\xi_{\|}$ is about 800 Å). A monolayer deposited on it is flat as well, except for some pinholes formed during deposition. For the 3, 5, and 7 ML films, one observes that $g_{N,N}(r)$ shows a linear dependence on $\log(r)$ for small r and saturates at large r. The corresponding r value at saturation increases with the increasing of the number of layers. This indicates that after the first monolayer, the subsequent layers start to fluctuate logarithmically. This is in accordance with the information in reciprocal space from the transverse scans. In addition, more holes are formed as the deposition proceeds, resulting in rougher interfaces.

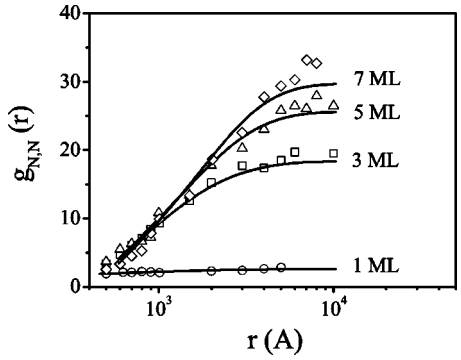

FIG. 5. The height-difference correlation function $g_{N,N}(r)$ for the surface of the samples obtained from the AFM measurements (symbols) along with the ones calculated by using the parameters listed in Table I (solid lines).

It is interesting to compare the obtained healing length ($\zeta=112\pm9$ nm) with the lateral correlation length ($\xi_{\|}=80\pm8$ nm) of the self-affine silicon substrate. The former is longer than the latter for our films such that the roughness arising from the substrate reduces rapidly as the film grows. At the same time, ripples on scales shorter than ζ are smeared out by the membrane over them. If ζ is much smaller than $\xi_{\|}$, the fluctuations replicated from the substrate persist. Sometimes the surface of the substrate scales in a logarithmic manner. If it happens that the scaling behavior of the substrate resembles the intrinsic one of the LB interfaces, one sees the asymptotic logarithmic scaling $g^{(\infty)}(r)$, even if the film is thin. However, if the coefficient of the logarithmic function for the substrate is different from the one for the intrinsic LB interfaces, one may observe a double-logarithmic scaling behavior. That is, the LB interfaces scale intrinsically on short length scales, but they may follow the fluctuation of the substrate on long length scales.

V. CONCLUDING REMARKS

The AFM and x-ray scattering results have shown that the interfacial morphology of imperfect LB films is determined by the competition between the roughening arising from pinholes and the smoothening due to elasticity of the membranes. The interfacial correlation function scales intrinsically in a logarithmic manner. However, the substrate plays a role in determining the actual morphology of the interfaces. The degree of vertical correlation in the LB films is a function of healing length. A rigid membrane with large healing length levels up the pinholes under it easily such that the subsequent membranes feel little influence of the pinholes. The vertical correlation length is therefore very short. On the other hand, if the interaction between the adjacent membranes is very strong, the subsequent membranes will be forced to follow the fluctuation of their predecessor, resulting in a high degree of vertical correlation. The interfacial morphology of an LB film with very short healing length is strongly influenced by the substrate, especially when the substrate is rough and the lateral correlation length of the substrate surface is long. At this time, the interfacial fluctuations of LB films will resemble to that of the substrate.

It should be pointed out that Eq. (4) is just a coarse-grained description of the growth dynamics of LB films. In most cases, the membranes would break up into macrodomains which, in turn, often consist of subdomains of submicrometer length scale representing microcrystalline aggregates.[27,28] The continuous growth equation assumes a smooth connection between the individual subdomains, ignoring the details near the edges of the domains so that it cannot account for the scattering from such boundaries. In

many practical x-ray diffuse scattering experiments, the momentum transfer $q_{\hat{x}}$ parallel to the interfaces spans a range from less than 10^{-3} nm^{-1} (limited by the instrumental resolution) to about 1 nm^{-1} (limited by the detectable intensity and the coherence length of the x rays). This corresponds in real space to a range of a few nanometers to several micrometers. The smooth connection hypothesis is justified in this sense. It does not apply to the diffuse scattering data at very large q_x.[29] The same is true when one treats the diffuse scattering near a Bragg point of (hkl), where $|h|+|k|\neq 0$.

Equation (4) does not apply to the case when membranes are very badly stacked. In addition, density fluctuations have been ignored. They have not yet been observed in the x-ray diffuse scattering experiments.[27] Finally, the thermal fluctuation of the membranes is not taken into account. An implication of this is that the fluctuations arising from pinholes dominate the thermally induced fluctuations. For a nearly perfect LB film, it might be better to use the correlation function for lamellar liquid crystals. Nevertheless, we believe that the correlation function in Eq. (5) can be applied to explain most of the x-ray diffuse scattering data of LB films. The quantities such as those given in Table I will certainly help us have a deeper understanding of the growth dynamics of the LB films.

ACKNOWLEDGMENTS

We thank Prof. L. Huang for the usage of the LB trough. This work has been supported by the Chinese Academy of Sciences and by the National Natural Science Foundation of China (Grant Nos. 10274096 and 10325419).

*Author to whom correspondence should be addressed; electronic address: mingli@aphy.iphy.ac.cn

[1] D. K. Schwartz, Surf. Sci. Rep. **27**, 241 (1997); G. G. Roberts, Adv. Phys. **34**, 475 (1985); R. H. Tredgold, *Order in Thin Organic Films* (Cambridge University Press, Cambridge, 1994).
[2] J. K. Basu, S. Hazra, and M. K. Sanyal, Phys. Rev. Lett. **82**, 4675 (1999); J. K. Basu and M. K. Sanyal, *ibid.* **79**, 4617 (1997); J. K. Basu and M. K. Sanyal, Phys. Rep. **363**, 1 (2002).
[3] P. Bassereau and F. Pincet, Langmuir **13**, 7003 (1997).
[4] V. Nitz, M. Tolan, J. P. Schlomka, O. H. Seeck, J. Stettner, and W. Press, Phys. Rev. B **54**, 5038 (1996).
[5] A. L. Barabasi, and H. E. Stanley, *Fractal Concepts in Surface Growth* (Cambridge University Press, Cambridge, 1995).
[6] A. C. Durr, F. Schreiber, K. A. Ritley, V. Kruppa, J. Krug, H. Dosch, and B. Struth, Phys. Rev. Lett. **90**, 016104 (2003).
[7] M. Seul and P. Eisenberger, Phys. Rev. A **39**, 4230 (1989).
[8] M. Tolan, in *X-Ray Scattering from Soft-Matter Thin Films*, Springer Tracts in Modern Physics (Springer, New York, 1998), Vol. 148.
[9] S. K. Sinha, E. B. Sirota, S. Garoff, and H. B. Stanley, Phys. Rev. B **38**, 2297 (1988).
[10] G. Palasantzas, Phys. Rev. B **48**, 14472 (1993).
[11] B. R. McClain, D. D. Lee, B. L. Carvlho, S. G. J. Mochrie, S. H. Chen, and J. D. Lister, Phys. Rev. Lett. **72**, 246 (1994).
[12] C. Holly and S. Bernstein, Phys. Rev. **49**, 403 (1936).
[13] S. Karmakar, and V. A. Raghunathan, Phys. Rev. Lett. **91**, 098102 (2003).
[14] M. Tolan, O. H. Seeck, J. P. Schlomka, W. Press, J. Wang, S. K. Sinha, Z. Li, and M. H. Rafailovich, and J. Sokolov, Phys. Rev. Lett. **81**, 2731 (1998).
[15] A. Gibaud, N. Cowlam, G. Vignaud, and T. Richardson, Phys. Rev. Lett. **74**, 3205 (1995).
[16] D. G. Stearns, J. Appl. Phys. **71**, 4286 (1992).
[17] D. G. Stearns and E. M. Gullikson, Physica B **283**, 84 (2000).
[18] M. Li, X. H. Li, L. Huang, Q. J. Jia, W. L. Zheng, and Z. H. Mai, Europhys. Lett. **64**, 385 (2003).
[19] S. F. Edwards and D. R. Wilkinson, Proc. R. Soc. London, Ser. A **381**, 17 (1982).
[20] M. Lutt, J. P. Schlomka, M. Tolan, J. Stettner, O. H. Seeck, and W. Press, Phys. Rev. B **56**, 4085 (1997).
[21] T. Salditt, T. H. Metzger, and J. Peisl, Phys. Rev. Lett. **73**, 2228 (1994).
[22] E. A. L. Mol, J. D. Shindler, A. N. Shalaginov, and W. H. de Jeu, Phys. Rev. E **54**, 536 (1996).
[23] A. Matsuda, M. Sugi, T. Fukui, S. Lizima, M. Miyahara, and Y. Otsubo, J. Appl. Phys. **48**, 771 (1977).
[24] L. Bourdieu, P. Silberzan, and D. Chaternay, Phys. Rev. Lett. **67**, 2029 (1991).
[25] S. W. Hul, R. Viswanathan, J. A. Zasadsinski, and J. N. Israelachvili, Biophys. J. **68**, 171 (1995).
[26] G. L. Gains, *Insoluble Monolayers at Gas-Liquid Interface* (Wiley, New York, 1966).
[27] R. Stommer and U. Pietsch, J. Phys. D **29**, 3161 (1996).
[28] Th. Geue, M. Schultz, U. Englisch, R. Stommer, U. Pietsch, K. Meine, and D. Vollhardt, J. Chem. Phys. **110**, 8104 (1999).
[29] T. Salditt, C. Munster, J. Lu, M. Vogel, W. Fenzl, and A. Souvorov, Phys. Rev. E **60**, 7285 (1999).